Template-Directed Synthesis of Oxide Nanotubes: Fabrication, Characterization, and Applications†

Changdeuck Bae,[‡,§] Hyunjun Yoo,[‡,§] Sihyeong Kim,[‡,§] Kyungeun Lee,[§] Jiyoung Kim,[||] Myung M. Sung,[⊥] and Hyunjung Shin*[,‡,§]

National Research Lab for Nanotubular Structures of Oxides and School of Advanced Materials Engineering and Center for Materials and Processes of Self-Assembly, Kookmin University, Jeongneung-Gil 77, Seoul 136-702, Korea, Department of Electrical Engineering, University of Texas at Dallas, Richardson, Texas 75080, and Department of Chemistry, Hanyang University, Seoul 133-791, Korea

Received July 31, 2007. Revised Manuscript Received November 13, 2007

A template-directed synthesis strategy is an ideal tool to fabricate oxide nanotubes in that their physical dimensions can be precisely controlled and monodisperse samples can be harvested in large quantity. The wall thickness of the oxide nanotubes is controllable by varying the deposition conditions, and the length and diameter can be tailored in accordance with the templates used. A wealth of functional oxide materials with the controlled polymorphs can be deposited to be nanotubular structures by various synthesis methods. This short review article describes the recent progress made in the field of the template synthesis of oxide nanotubes. We begin this review with the comprehensive survey on the research activities of the template-directed oxide nanotubes. We then focus on the template synthesis that combines porous membrane templates with various deposition techniques and discuss the processing issues associated with coating inside nanoscale pores, selective etching of oxide nanotubes from the templates, and dispersion against the formation of nanotubes' bundle-up. Structures and physical properties of the oxide nanotubes prepared by template synthesis are also summarized. Their potential for application in drug-delivery systems, sensors, and solar energy conversion devices, which could be facilitated by the template synthesis, is discussed. Finally, we conclude this review as providing our perspectives to the future directions in the template-directed oxide nanotubes.

1. Introduction

A template-directed approach to preparing nanomaterials has been pioneered by Martin and his co-workers since the early 1990s[1] in which the synthesis of uniform-sized nanomaterials benefits from the use of membrane templates with the monodisperse cylindrical pores in terms of the diameter and length. The timely discovery[2] of carbon nanotubes (CNTs) by Iijima triggered many researches and studies on CNTs[3,4] as well as other one-dimensional (1-D) nanomaterials, such as polymer,[5] metal,[6] and ceramics,[7–10] with tubular structures. Among 1-D nanomaterials, tubular-structured materials have shown unique chemical and physical properties because of their outer as well as inner surfaces having the "wall" of nanometer thick. Nanotubular structures of inorganic oxides are, in particular, receiving a great deal of attention because of their potential for newly emerging applications in drug-delivery systems,[11] molecular separation,[12] single-DNA sensing,[13] pollutants decomposition,[14] hydrogen fuel,[15] gas sensors,[16] and solar energy conversion devices.[17–19] The applications employ the inherent characteristics of oxide nanotubes that involve hollow core structures, ultralarge specific surface areas, very narrow inner pores, and catalytic surface properties.

There are a number of reports on the synthesis strategies of the nanotubular structures of oxide materials in the literature. About 50 years ago, Nemetschek and Hofmann reported that the silica nanotubes are generated by the reaction of silica and silicon at high temperature.[20] Such templateless, spontaneous formation of oxide nanotubes is also found elsewhere, for instance, by hydrothermal treatment of ceramic powders or films[8] and other methods.[21] Here in this short review article, we focus on the synthesis of oxide nanotubes by the templating method instead of the templateless synthesis. Although the templating method limits the dimensions of nanotubes by the dimensions of the templates, it has many more advantages over the templateless methods, for example, facile fabrication, various compositions of materials, and uniform sizes of the formed nanotubes. Therefore, template-directed methods can allow us to have manufacturing ability to produce monodisperse 1-D nanotubular-structured materials with a significant high yield for the future nanodevices. We can categorize the fabrication methods for all of these oxide nanotubes in terms of template types and synthesis methods to deposit materials onto the templates. Scaffolds used can be mainly divided into three types: positive templates, negative templates, and quasi-templates. Positive templating is using 1-D nanostructures

† Part of the "Templated Materials Special Issue".

* To whom correspondence should be addressed. E-mail: hjshin@kookmin.ac.kr.

‡ National Research Lab for Nanotubular Structures of Oxides and School of Advanced Materials Engineering, Kookmin University.

§ Center for Materials and Processes of Self-Assembly, Kookmin University.

|| University of Texas at Dallas.

⊥ Hanyang University.

10.1021/cm702138c CCC: $40.75
Published on Web 01/19/2008

Table 1. Template-Directed Methods to Preparing Oxide Nanotubes

methods		oxide materials	dimensions (nm) ($t_w/D_i/D_o/L$)[a]	ref
quasi-template synthesis	electrospinning	TiO_2, ZrO_2, SiO_2	50–100/20–360/100–500/-	22, 54, 88
	anodization	TiO_2, ZrO_2, TiO_2-Nb_2O_5, zirconium titanate, Al_2O_3	5–70/12–150/35–250/ 500–22000	10, 16, 18, 52, 53
	dynamic mineralization	SiO_2	1.4/22/27/3000	56
positive template synthesis	solution-based deposition	TiO_2, ZrO_2, SiO_2	5–100/30–300/3–300/>100	23, 31, 32, 37
	CVD	SiO_2	80–100/100/300/1000–3000	33
	pulsed laser deposition	$BaTiO_3$, PZT	5–20/20–150/200–1000	36
	electrochemical deposition	TiO_2	25–50/50–100/120–180/8000	7
	heat treatments	SiO_2, $ZnAl_2O_4$, Bi_2O_3	10–100/30–100/50–200/ >5000	24, 25, 35
	biomineralization	TiO_2, SiO_2	3–50/5–200/10–600/ 50–10000	27, 39–42
	ALD	Al_2O_3	5–50/30–300/35–300/>500	29
negative template synthesis	solution-based deposition	TiO_2, MnO_2, V_2O_5, Co_3O_4, ZnO, SiO_2, WO_3, In_2O_3, Ga_2O_3, $BaTiO_3$, $PbTiO_3$	3–100/30–300/30–300/ 500–60000	8, 11, 12, 14, 43
	ALD	TiO_2, ZrO_2, Al_2O_3	2–100/30–300/30–300/ 500–60000	28
	water-induced vapor deposition	SiO_2	2–100/30–300/30–300/ 500–7000	89

[a] t_w = wall thickness, D_i = inner diameter, D_o = outer diameter, and L = length.

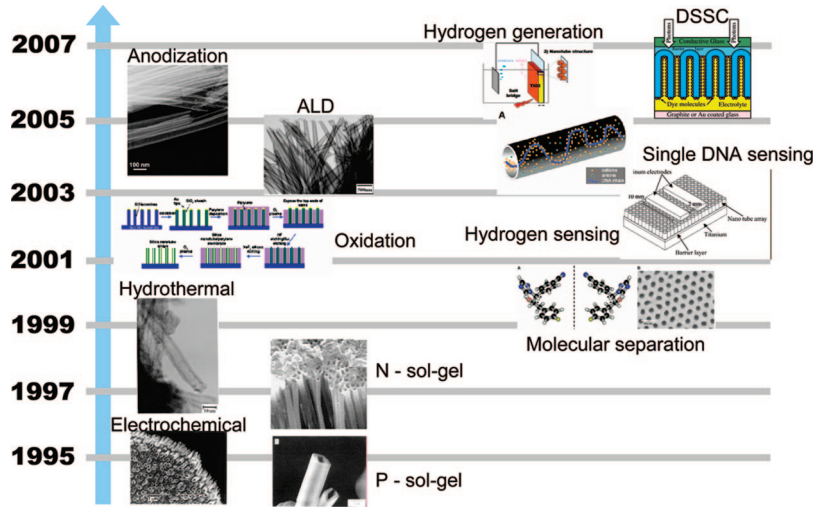

Figure 1. Schematic chart that briefly shows the historical survey on the synthesis (left) and applications (right) of oxide nanotubes. Left: P sol–gel, electrochemical, N sol–gel, hydrothermal, and oxidation methods are respectively reproduced from refs 31a, 7, 8a, 9a, and 24 with permission. Copyright 1995–2003 American Chemical Society; ALD and anodization methods are from refs 28a and 10f with permission. Copyright 2004–2005 Wiley InterScience. Right: Molecular separation from ref 12 with permission. Copyright 2002 American Association for the Advancement of Science; hydrogen sensing from ref 16a with permission. Copyright 2003 Elsevier BV; single-DNA sensing, hydrogen generation, and DSSC respectively from refs 13, 15, and 18c with permission. Copyright 2005–2006 American Chemical Society.

such as nanowires, nanorods, and CNTs in which oxide materials are coated on the outer surfaces of the template. Subsequently, they are removed by chemical etching and/or pyrolysis. Porous membranes with monodisperse cylindrical pores are used as negative templates that involve anodic aluminum oxides (AAOs, or, depending on the authors, porous anodic alumina or porous aluminum oxide) and track-etched polymers [mostly, polycarbonate (PC)] and of which oxide materials are deposited on the surfaces of their inside pores. Furthermore, the formation of oxide nanotubes by anodization of metal foils or films[9] and electrospinning[22] can be assorted quasi-templating methods in that the guiding strategy facilitates the synthesis rather than being shaped into the physical templates. In addition to the template types, deposition methods to coat the templates may simplify to subdivide the template-directed oxide nanotubes. They include electrochemical deposition,[6] sol–gel synthesis,[7,23] oxidation,[24–26] biomimetic mineralization,[18,27] and gas-phase atomic layer deposition (ALD),[28–30] and all are summarized in Table 1.

Here we offer a comprehensive review on the template-directed oxide nanotubes in terms of synthesis strategy, characterization and properties, and potential applications (see Figure 1). We begin with brief survey on the research activities of the template-directed oxide nanotubes and then focus on the oxide nanotubes that have been prepared with a combination of porous membrane templates with various materials deposition techniques, such as sol–gel, electrochemistry, and ALD. We also discuss the processing issues related with nanopore coating, selective etching, and disper-

sion and summarize the structural and physical properties of the oxide nanotubes fabricated by template-directed synthesis. Applications of oxide nanotubes, facilitated by the template synthesis, are also discussed, with a potential in drug-delivery systems, sensors, and photovoltaic devices. We conclude this review with personal perspectives on the future directions in the fundamental studies as well as potential applications using the template-directed oxide nanotubes.

2. Synthesis Strategy of Template-Directed Oxide Nanotubes

2.1. Use of Positive Templates. CNTs were used for the first time as the positive templates in the fabrication of oxide nanotubes. Nakamura et al. demonstrated that amorphous silica nanotubes can be synthesized by Stöber sol–gel deposition on the surfaces of CNTs under the presence of DL-tartaric acid, followed by their burning.[31] A similar concept was also applied to the formation of yttria-stabilized cubic zirconia.[32] Vertically aligned, relatively short CNTs were covered with silica using plasma-enhanced chemical vapor deposition (CVD), producing silica nanotube arrays after thermal oxidation.[33] Hoyer showed that arrays of titania nanotubes can be fabricated by electrochemical deposition on the surfaces of poly(methyl methacrylate) nanorod arrays, followed by dissolution of the polymer cores that have been replicated from AAO templates and used as positive templates.[7] Recent studies[34] on the coating of thin dielectric layers on the surfaces of CNTs using ALD, in principle, show the feasibility that these coaxial nanotubes can be transformed to fine oxide nanotubes after calcination.

Employing nanowires or nanorods as positive templates is also a reasonable way to fabricate oxide nanotubes, which could be well-dispersed without any bundle-up and array structures when the nanowires are arrayed. For example, the Yang group have developed a strategy that silica nanotubes are created by thermal oxidation of silicon nanowires followed by selective chemical etching of the Si core wires.[24] Heat treatments might lead to another hollow structure even without the removal step of core materials. Fan et al. reported that $ZnO@Al_2O_3$ core/shell nanowires can be transformed into a $ZnAl_2O_4$ spinel structure of nanotubes after annealing at the appropriate temperature in which the core materials are diffusively consumed through the Kirkendall effect.[35] Li et al. also reported Bi_2O_3 nanotubes from Bi nanowires, exactly, the $Bi@Bi_2O_3$ core/sheath system for which the detailed formation mechanism is still unclear.[25] Solution-based deposition of thin oxide layers onto the surfaces of soluble nanorods and subsequent etching of the cores result in oxide nanotubes. Murphy, Caruso, and co-workers have demonstrated that metal nanorods can serve as sacrificial templates, yielding silica and titania nanotubes after selective etching of the core rods.[23a,b] Sol–gel-processed TiO_2 and Al_2O_3 nanotubes were also reported via ZnO nanowire templating. Ferroelectric nanotubes such as barium titanate ($BaTiO_3$) and lead zirconate titanate (PZT) were recently demonstrated by depositing thin ferroelectric oxide layers with pulsed laser deposition using Si and ZnO nanowires as positive templates.[36] Electrospun poly(L-lactide) fibers also served as positive templates in order to produce TiO_2 nanotubes.[37]

Combining the positive template strategy with ALD, the formation of oxide nanotubes with controllable wall thickness has recently been reported by many researchers. Positive templates used were ZnO nanorods, self-assembled polystyrene-*block*-poly(4-vinylpyridine) block copolymer nanorods, electrospun poly(vinyl alchol) fibers, and tris(8-hydroxyquinoline)gallium nanowires, and Al_2O_3 nanotubes were prepared by ALD with trimethylaluminum and water as source materials after chemical etching, thermal decomposition, or dissolution of the organic cores.[29]

In addition to the typical materials synthesis approaches, nature provides a slow yet robust strategy in the formation of oxide nanotubes. In nature, it is known that the specific molecules induce to condensate biominerals on their surfaces.[38] By adopting this principle, researchers produced oxide nanotubes by condensation of the precursor species on the surfaces of fibrils or tubules of biomolecules and their subsequent burn-out. Lipid, surfactant, peptide, and virus fibrils were typically used as templates, generating fine silica nanotubes after calcination.[27] Organogelators are also employed for the formation of helical nanotubular structures by sol–gel condensation of titanium, tantalum, and vanadium alkoxides.[39] Recently, Ji et al. reported that tetraethoxysilane (TEOS) molecules can be condensed on both the inner and outer surfaces of peptidic lipid nanotubes, resulting in double-wall silica nanotubes.[40] Jung et al. also reported that double-wall TiO_2 nanotubes can be achieved by condensing $Ti(O\text{-}i\text{Pr})_4$ precursors onto both surfaces of the self-assembled organogel tubes.[41] Rare-earth oxide nanotubes were also achieved by templating the self-assembly of dodecylsulfate surfactant molecules.[42]

In positive templating, the inner diameters and the length of the resulting oxide nanotubes are respectively decided by the outer diameters and the length of the original 1-D templates and the outer diameters are responsible for the deposited wall layers. Although these approaches give us relatively facile processes in the synthesis of oxide nanotubes with controlled diameters, additional process steps are required to obtain oxide nanotubes having uniform length and open ends, for instance, reactive ion etching and mechanical polishing for vertically arrayed samples.

2.2. Use of Negative Templates. *2.2.1. Solution-Based Synthesis.* Negative templating approaches using porous membranes often offer excellent size uniformity in the diameter and length of the formed oxide tubes on a nanometer scale. In principle, deposition methods used in positive templating can be applied to the negative template processes. Lakshmi et al. formed sol–gel titania nanotubes using AAO membranes as negative templates. In their experiments, the formation of oxide walls on the surfaces of inner pores was controlled by the exposure time of titanium isopropoxide precursors.[8a,b] Michailowski et al. have synthesized highly arrayed TiO_2 nanotubes possessing a thin wall layer using a thermal decomposition process with $Ti(O\textit{i}Pr)_4$.[8i] Fisher, Samulski, and others reported In_2O_3 and Ga_2O_3 nanotubes as well as perovskite nanotubes of $BaTiO_3$ and $PbTiO_3$ by using a sol–gel protocol.[8j,k] In the solution-

based processes, there unambiguously exists a trade-off between the deposition of thin wall layers and the formation of continuous films and it impedes precise control of the formation of wall layers. The Martin group has employed an ultrasound-assisted sol–gel process to improve the nanopore diffusivity of the TEOS precursors and, hence, the uniformity of thin wall layers of silica nanotubes.[81] Recently, Kovtyukhova et al. have introduced a layer-by-layer method based on the solution phase, called the "surface sol–gel process", for the formation of silica nanotubes in a controlled manner.[43]

In addition to the monodispersity of oxide nanotubes, the ability to produce a thin as well as controllable wall layer of oxide nanotubes would allow for better applications using their electrical and optical properties. For instance, the optical properties of semiconductor oxide nanotubes could be sharply changed in the range of a few nanometers in one direction because of the quantum-size effect.[44,45] Furthermore, their electrical conductivity can be sensitively perturbed by accumulation[16] or depletion[46] of electrical carriers when additional molecules are absorbed onto the surfaces of the thin oxide layers.

2.2.2. Vapor-Phase Synthesis. Considering the use of negative templates combined with a gas-phase materials deposition technique, most of the physical depositing techniques are suffering from the direct line-of-sight to coat the inner pores. They have usually shown poor conformal coating onto high aspect ratios of the negative templates. Metal−organic CVD techniques were employed for fabricating copper oxide, nickel oxide, and indium oxide nanotubes where AAO membranes served as high-temperature-stable templates.[47] The resultant nanotubes with a relatively short length compared to the original templates used were obtained as a result of incomplete conformal coating, but it would likely be improved with appropriate deposition conditions. ALD, a variant of CVD, is a recently developed deposition technique of thin film materials in the semiconductor industry using a self-terminating surface reaction, hence allowing excellent conformal coatings, even on most of the negative templates with a high aspect ratio. It relies on sequential saturated surface reactions, which result in the formation of a monolayer in each sequence. The successive self-terminating growth mechanism in ALD inherently eliminates reactions in the gas phase. Elimination of gas-phase reactions results in the greater relative importance of surface reactions. Shin, Kim, and co-workers have shown negative templating with the ALD technique in order to fabricate TiO_2 and ZrO_2 nanotubes with controllable dimensions with respect to the diameter and length as well as their wall thickness.[28a] That is, the outer diameter and length of the tubes are decided by the original template used, and the wall thickness and inner diameter are tailored simply by the number of deposition cycles with subangstrom precision. Independently, Sander et al. conducted ALD of TiO_2 on the highly ordered AAO as a template and obtained TiO_2 nanotubes.[28b] Recently, this strategy has been applied to the formation of ferromagnetic nanotubes,[48] nanostructured photocatalytic surfaces,[49] physical confinements for nanowire growth,[50] and DSSCs.[18e]

In a typical fabrication, porous membranes with the track-etched or anodized cylindrical pores having either one or both sides open can be used as templates. Both AAO and PC membranes are commercially available, but homemade AAO templates are often used for the purpose of obtaining desired template dimensions (i.e., uniform sizes in length and pore diameter) and enhanced surface morphology compared to the track-etched pores.[28] Once thin oxide layers are deposited onto the porous template, mechanical polishing or similar treatments for the removal of undesired layers sitting on the membrane face(s) might be indispensable in order to harvest free-standing oxide nanotubes upon removal of the templates.[28b]

Use of PC Templates. Shin et al. have introduced octadecyltrichlorosilane (OTS)-self-assembled monolayers (SAMs) by microcontact print (μCP)[51] on the faces of a PC template as a releasing layer and enhanced the collection yield of free-standing oxide nanotubes upon dissolution of the template.[28a] In the strict sense, such a treatment does not produce SAMs on the polymeric template and is not resistant to materials deposition. Oxide films deposited onto the OTS-treated surfaces after a certain number of consecutive ALD coating cycles are observed in electron micrographs before dissolution of the template. Although complete selective ALD coating of oxides only onto the inner pores is not achieved in all cases where PC membranes are used as templates, free-standing cylindrical nanotubes can still be collected completely after dissolution of the templates without any additional polishing step. We suspect that, in this case, OTS molecules did not form SAMs and are rather physisorbed on the PC surfaces, forming a shell layer consisting of OTS molecules hydrolyzed and/or polymerized in ambient air. Therefore, oxide films deposited on the organic layer can be easily disintegrated during dissolution of the PC template in chloroform. Accordingly, the surface treatment step with OTS molecules makes it possible to fabricate free-standing structures of oxide nanotubes without any further process.

Figure 2 shows the typical topology of several kinds of oxide nanotubes prepared by ALD using the track-etched membrane, i.e., PC, as a negative template. Brief procedures for Al_2O_3 nanotubes are as follows: Anhydrous hexane solutions containing 0.1 mM OTS were coated onto the surface of the poly(dimethylsiloxane) (PDMS) stamp by spin-coating at 2000 rpm for 30 s; the OTS molecules on the PDMS stamps were transferred onto both surfaces of either a PC membrane by a standard μCP procedure for about 15 s; trimethylaluminum was used as a source of aluminum; water vapor was used as an oxidant; argon was used as a carrier gas and for purging; individual alumina nanotubes deposited onto the PC membranes were released from the template by dissolving it in chloroform. Free-standing, monodisperse alumina nanotubes are clearly shown in the scanning electron microscopy (SEM) image of Figure 2c. The SEM image of Figure 2c shows hollow nanotubular structures with uniform thickness, as confirmed by transmission electron microscopy (TEM) results. The tube length of $\sim$7 μm corresponds to the thickness of the original PC membranes, implying that a highly uniform and conformal coating was successfully achieved. The relatively rough surface morphology of the

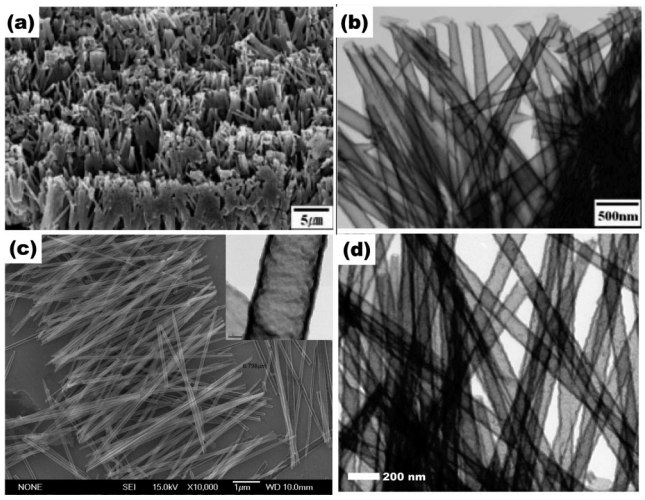

Figure 2. Various functional oxide nanotubes prepared by the template-directed ALD process with a PC membrane. (a) SEM of TiO_2 nanotubes produced in large quantity by the template synthesis. (b) TEM of ZrO_2 nanotubes fabricated by the same method as that in part a. Adopted from ref 28a with permission. Copyright 2004 Wiley InterScience. (c) SEM and (d) TEM of well-dispersed Al_2O_3 nanotubes. The inset in part c shows the morphology of as-deposited alumina nanotubes created by this method.

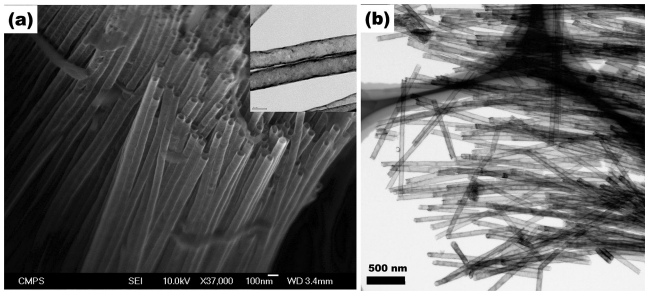

Figure 3. Typical electron micrographs of TiO_2 nanotubes that have been produced by the template-directed ALD process with AAO membrane. (a) SEM and (b) TEM of TiO_2 nanotubes with high aspect ratios and smooth surfaces.

resulting tubes originated from the pore surfaces of the track-etched PC membranes as shown in the inset. Bottleneck-like variations in the nanotube diameter along the tube axis also arose from the original templates that were created by an effect on the surfactants in faster etching conditions.

Use of AAO Templates. In the case of the employment of a porous alumina membrane as the template, smooth surfaces as well as a uniform diameter in the axis of the resulting oxide nanotubes could be obtained. The same approach was applied to the AAO templates. Both sides of the alumina membrane were treated with UV ozone to render them hydrophilic. OTS molecules were then transferred onto both sides of the surfaces of the template by μCPs and SAMs formed on the surfaces. After contact printing, the surfaces of the template were washed with chloroform to remove any excess molecules physisorbed upon the OTS-SAMs, thus exposing chemically inert methyl surfaces. During the ALD process, OTS-SAM layers functioned as resistant layers to materials deposition. Mechanical polishing or dry etching could also possibly be applied to the removal of the undesired oxide layers deposited on both faces of the template.

Figure 3 exhibits typical electron micrographs of TiO_2 nanotubes that have been fabricated by ALD coating with homemade AAO membranes as templates. Monodisperse titania nanotubes with ~60 nm diameter, ~15 nm wall thickness, and an aspect ratio of ~150:1 are shown. The overall structural quality of oxide nanotubes such as surface morphology and diameter uniformity seems to be better than that prepared with the PC template. Note that the nanotubes were obtained after etching of the AAO template bundle-up, as shown in the SEM of Figure 3. The formation of bundles is common to the AAO-directed synthesis of oxide nanotubes, as is generally described in the literature. The pore size effect on the ALD coating, selective etching from the oxide templates, and bundle formation will be discussed later.

2.3. Use of Quasi-Templates. There are other notable methods for making oxide nanotubes, which we here categorize into quasi-templating methods. Anodization of metal foils or films in an acidic solution under appropriate experimental conditions leads to the formation of individual tubular structures of metal oxides. An anodized Ti surface, in particular, has been extensively investigated. Since the first observation by Zwilling et al.,[10a] Schmuki, Grimes, and co-workers have extensively exploited such a system and made significant progress, even demonstrating titania nanotubes having smooth surface morphology and high aspect ratio (several hundreds of micrometers in length) for potential applications such as photovoltaics and sensors.[10] Zirconium oxide, $TiO_2-Nb_2O_5$, and zirconium titanate nanotubes were also recently demonstrated using such a method by the Schmuki group.[52] Individual alumina nanotubes were also observed in anodized Al surfaces by Pu et al.[53]

Unprecedentedly, long nanotubes can be directly prepared by cospinning of organometallic precursors and microfluids of oil, in principle without maximum length limits. Xia and Li have recently reported titania nanotubes that were fabricated by coaxial electrospinning of a ethanolic mixture of poly(vinylpyrrolidone) and $Ti(OiPr)_4$ and heavy mineral oil, followed by calcination.[22] Larsen and his co-workers also independently demonstrated zirconia nanotubes by using a solution of zirconium acetate in acetic acid and olive oil as cospinning agents.[54]

Nesper and co-workers reported that hydrolysis of vanadium oxide precursors and, in turn, hydrothermal treatments in the presence of ligand molecules produce multiwall vanadium oxide nanotubes, which consist of highly crystalline shell layers of vanadia separated by organic amine layers.[55] In a recent publication on the biomimetic mineralization process, Pouget et al. reported the formation of double-wall silica nanotubes and proposed that they are mineralized through the so-called dynamic templating process rather than the preassembled supramolecules.[56]

3. Processing Issues of Membrane Templating

3.1. Coating of Nanopores. The fabrication of oxide nanotubes using membrane templates offers superior controllability to all of their physical dimensions, i.e., wall thickness, length, and diameter. To this end, the template-directed process with porous membranes might be tempting and is expected to be used as a general tool to prepare oxide nanotubes.

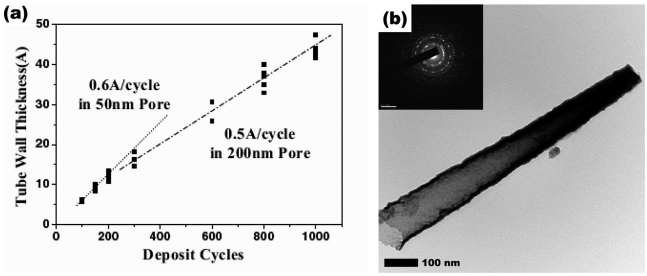

Figure 4. (a)Growth rate as a function of the nanopore diameter. Reproduced from ref 28a with permission. Copyright 2004 Wiley InterScience. (b) TEM image of a part of the ZrO_2 nanotube. Inset: Typical electron diffraction patterns of ZrO_2 nanotubes recorded from part b, indicating a tetragonal polymorph.

Although solution-based deposition processes offer opportunities to be applicable to a variety of oxide materials in the synthesis using porous membranes, they mostly involve a difficult-to-control procedure with respect to wall thickness in the formation of nanotubular structures. This is because tubular structures of oxide materials are formed after complete gelation of colloidal sols into the continuous films. Otherwise oxide nanotubes with walls of discontinuous films would be often made upon removal of the templates. The surface sol–gel process allows the coating of dense and continuous oxide layers, and thus improved production of template-directed oxide nanotubes, but it involves a quite slow process.[43]

In addition to the deposition of sol particles into nanopores, the insertion of other materials such as magnetic colloids, biomolecules, and light-harvesting species would make oxide nanotubes useful. Controlled capillary insertion of materials into nanoscale pores has been the focus because of fundamental interests as well as for practical applications. In an early work, Ugarte et al. observed that molten silver nitrate was filled into CNTs with inner pores as small as 4 nm by capillary forces.[57] In the oxide nanotube systems, English and co-workers investigated the diffusion in hydrophobic inner pores of template-synthesized silica nanotubes and observed relatively slow diffusion.[58] Fan et al. demonstrated that silica nanotubes prepared by positive templating can be employed as nanofluidic channels during single-DNA translocation.[13]

In gas-phase synthesis, there are some aspects of the coating onto the inner pores with the nanometer scale to be considered. George and co-workers reported that the exposure time of reactant molecules during the ALD process was of importance to conformal and complete coating inside nanopores with a high aspect ratio.[59] They also confirmed the results by conducting a calculation considering the mean free path of reactant molecules in the ALD system. Indeed, in a typical ALD condition, the reactant molecules have a mean free path of approximately micrometers.[60] Such a length scale is indicative that the mean free path is effective when coating inside nanopores. The effect of highly curved surfaces of nanopores is also unambiguously operating in the formation of oxide nanotubes by ALD. Shin et al. have reported that there is faster growth rate of TiO_2 nanotubes in pores of 50 nm diameter than in pores of 200 nm diameter.[28a] Figure 4 is a graph of the growth rate versus pore diameter that has been collected from a series of TiO_2 nanotube samples. The growth rate of the wall thickness of the TiO_2 nanotubes was linear with a function of ALD cycles, as plotted in the inset of Figure 4a. The growth rates were 0.6 and 0.5 Å per cycle for PC templates of 50 and 200 nm diameters at 130 °C, respectively.

It is also noteworthy that the growth rates increase with a decrease in the pore diameter of the templates. Lower absorption of the precursors to the surfaces of the nanopores than to the planar surfaces competes with the pressure differences between the different pore sizes in the templates; a smaller pore size shows a higher growth rate for the wall of the tubes. This leads to the dependence of the growth rate on the pore diameter. Exact mechanisms are not clearly understood, but there would a few possible explanations. George and co-workers reported that during low-temperature ALD of Al_2O_3 water used as an oxidant remained condensed on the surfaces.[62] Condensed water facilitated by nanopores would be a possible source for the faster growth of nanotubes. Another explanation is the increased stress at highly curved surfaces for the deposition of oxide nanotubes. Figure 4b shows TEM results of a ZrO_2 nanotube that has been deposited by ALD with the PC template. TEM image exhibits the tube wall with a thickness gradient ranging from 8 to 30 nm. Note that the diameter of a ZrO_2 nanotube varies from 120 to 60 nm, indicative of the bottleneck shape of the original PC template. In the same pore, different growth rates also imply that stress is involved in the thin film deposition at higher curvature. The crystal structure of as-deposited ZrO_2 nanotubes also supports the effect of stress. The electron diffraction pattern shows that the crystalline ZrO_2 nanotubes have a tetragonal polymorph. The presence of tetragonal zirconia nanotubes without any stabilizers at room temperature might be reasoned by increased stress at the curved surfaces.

3.2. Selective Etching and Dispersion of Oxide Nanotubes from the AAO Template. Inorganic oxide nanotubes obtained from PC templates were mostly free-standing, as shown earlier, because the PC template, compared to AAO, can be rapidly dissolved by organic solvents. In contrast, in the case of using AAO as templates, it is quite difficult to obtain individual nanotubes. However, the use of an AAO membrane as a template still offers several advantages when employed in our strategy: AAO has a pore density ($\sim 10^{11}$ cm^{-2}) more than 2 orders of magnitude higher than that ($\sim 10^{9}$ cm^{-2}) of PC, it can be applied at higher temperatures, and nanotubes obtained from a porous alumina template have smoother surface morphology than those from a PC template. Accordingly, there is a trade-off in choosing template materials. From the Pourbaix diagram for alumina,[63] we find that tube materials that can be applied to this strategy are limited. Because alumina dissolves either under ~pH 4 or over ~pH 9, we should either choose tube materials that are stable under these conditions or use a different pH value for alumina dissolution. Recently, Xiong et al. investigated the structure of anodized alumina prepared using a solution of oxalic acid and observed the presence of aluminum oxalate by UV Raman spectroscopy.[64] Their study

implies that pure alumina nanotubes might be separated from the porous alumina template with the template-directed ALD methods.

In principle, free-standing, individual oxide nanotubes can be obtained to be released from the porous alumina template by dissolving the template selectively as well as completely. However, we often find the bundle structures consisting of oxide nanotubes in the literature as well as our experiments. Figure 5a shows a representative TEM image of a bundle of TiO_2 nanotubes. Once suspended aggregates of oxide nanotube bundles are formed, it is impossible to in high yield separate nanotubes from each other without damages even under ultrasonic irradiation. We suspect that the assembly into the bundle of the nanotubes was driven by strong lateral capillary forces[65] between nanotubes having hydrophilic surfaces. Such an assembly can occur during drying of residual solvents from the surfaces of the nanotubes as well as during the dissolution of alumina in an aqueous etching solution. When alumina is dissolved, an interface between the etching solution and the concentrate of the species dissolved molecularly from alumina is instantly created between the surfaces of oxide nanotubes, as depicted in Figure 5b. As the area of the curved interfaces between tubes decreases as a result of minimization of the interfacial free energy of the interfaces between the etching solution and the concentrate, the oxide nanotubes move into contact with one another, producing bundles of nanotubes. This fluid−fluid interface is strong enough to yield an assembly of even centimeter-scale objects.[66] Moreover, once the capillary-driven organization is formed, it is irreversible, even under ultrasonic irradiation.[67] The formation of bundles seems to hinder the fabrication of advanced nanodevices or systems that utilize the novel nanotubular structure of oxides.

On the other hand, we also see well-dispersed 1-D nanomaterials that have been prepared by the template-directed strategy in the literature. We found that, in the case of good dispersion of the templated nanomaterials, they mostly have supporting films in their contact that have been used during electrochemical deposition as electrodes. In that case, although the bundles of nanomaterials were formed after etching of the template, their roots in contact with the supporting films are apart. These structures seem to improve dispersion of the templated nanomaterials. We adopted this strategy and obtained good dispersion results. Figure 5c shows well-dispersed TiO_2 nanotubes that have been attached to Pt films of ~200 nm deposited by sputtering. To investigate the dispersion yields of oxide nanotubes, we coated an aqueous solution containing TiO_2 nanotubes on a Si wafer and observed their dispersion on the wafer after complete drying of the solvent. There were no bundles and aggregates in an approximately square centimeter region to date as shown in Figure 5c, implying the preparation of ideal suspensions of oxide nanotubes.

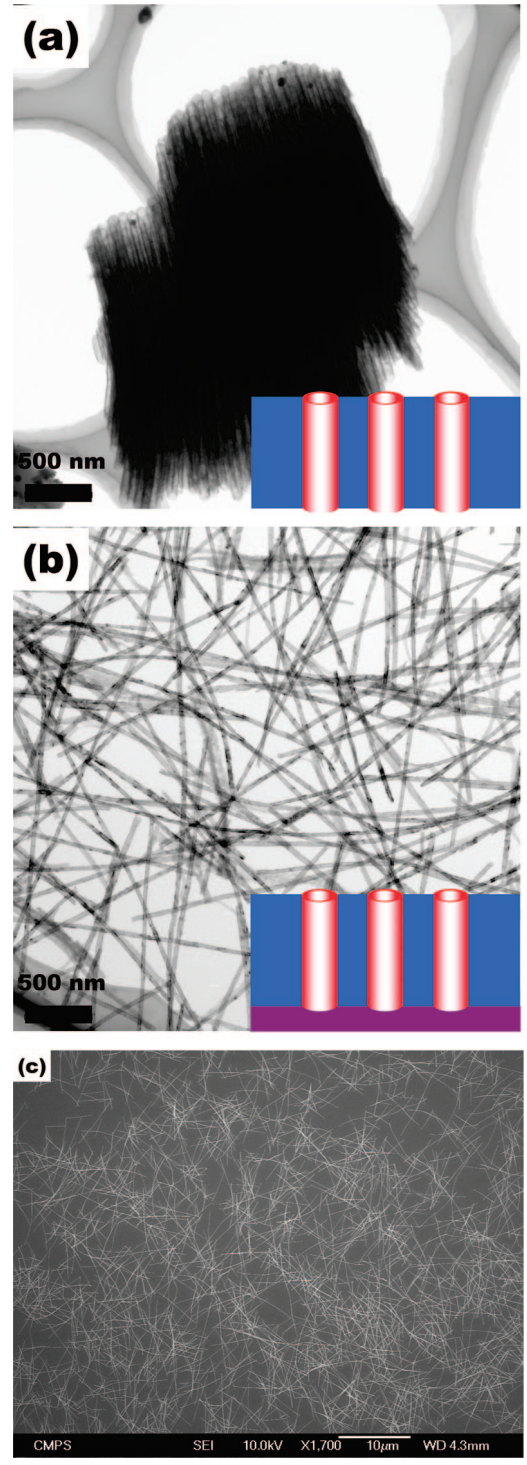

Figure 5. (a) Typical TEM of bundles of titania nanotubes after etching of the surrounding alumina templates. Inset: Schematic depiction for explaining the mechanism of the bundle formation of the oxide nanotubes: A fluid−fluid interface between the etchant and the dissolved concentrate is instantly created; the liquid–liquid interface is wet at the hydrophilic oxide surfaces of the nanotubes, forming a concave meniscus; the oxide nanotubes move into contact to minimize the interfacial free energy; this interface exists during the dissolution of alumina. (b) Typical TEM of well-dispersed, individual titania nanotubes after etching of the template. The dispersion was carried out under ultrasound irradiation for 3 min in pure water, with the supporting Pt (200 nm) films on the nanotubes. (c) SEM of TiO_2 nanotubes coated in a large area.

4. Characterization

The application of oxide nanotubes is dependent upon their fundamental chemistry and physics associated with electron transport properties, optical properties, nanopore wetting, and crystallinity. In this section, we discuss the physical proper-

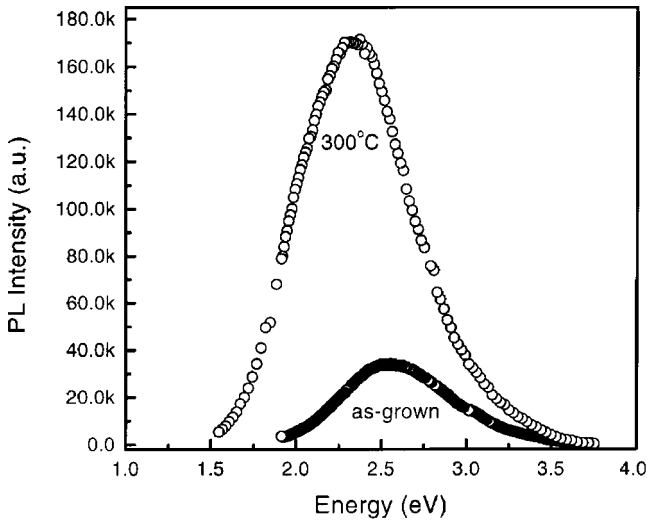

Figure 6. Photoluminescence spectra taken from template-synthesized sol–gel silica nanotubes. The wall thickness, average diameter, and length were 3–7 and 30–50 nm and 100 μm, respectively. These blue and green emissions were expected to be originated from the Si−OH complex on a large number of surfaces of silica nanotubes. Reproduced with permission from ref 77. Copyright 2002 American Institute of Physics.

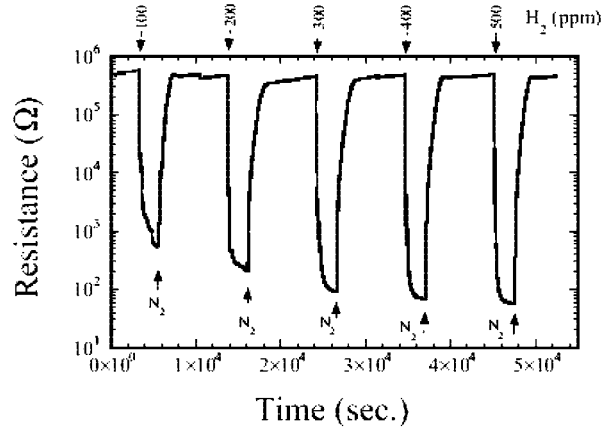

Figure 7. Resistance changes of anodized TiO_2 nanotube arrays under different hydrogen concentrations at 290 °C. The inner pore diameter, wall thickness, and length were 22, 13, and 200 nm, respectively. Reprinted with permission from ref 16b. Copyright 2003 Wiley InterScience.

ties of oxide nanotubes that have been prepared by the template-directed processes.

4.1. Electrical Properties. Nanoarchitectured metal oxide structures might exhibit the unusual transport properties of electrical carriers compared to their bulk counterparts. Unexpected conductance changes of a few orders of magnitude have been reported in several nanocrystalline metal oxides.[68] Upon the emergence of applications such as gas sensors, biosensors, hydrogen fuels, and DSSCs, the electron transport properties of nanotubular structures of oxide materials have received increasing attention and thus need to be done. Grimes and co-workers reported a change of 10^4 in electrical conductance upon exposure of hydrogen at 290 °C to anodized TiO_2 nanotube arrays and attributed this to modulation of the space charge layers as a result of hydrogen absorption on the surfaces of the nanotubes (Figure 7).[16] Although the exact resistivity of the individual, anodized TiO_2 nanotubes is not known because of the formation of the Schottky barrier, one could expect that they have a much smaller value of resistivity compared to that of bulk titania.

Kim and others recently investigated the electron transport properties of a single TiO_2 nanotube by using a nanomanipulator with a fully equipped focused ion beam. They reported a resistivity on the order of 1 Ω cm,[69] which was extremely lower than that of stoichiometric bulk TiO_2 ($\sim 10^8$ Ω cm).[70] This result was responsible for the undesired factors such as Ga ion beam damage and Pt contamination during the experiments. Recently, our group has studied the electrical characteristics of TiO_2 nanotubes via high-voltage measurements. The TiO_2 nanotube arrays were fabricated by the template-directed ALD, and stoichiometric TiO_2 nanotubes were obtained without any contaminants. We considered several important parameters such as the Schottky barrier height[71] and the contact security of the devices[72] to clarify the results. The resistivity values of individual TiO_2 nanotubes ranged from 50 to 100 kΩ cm. This value is about 3 orders of magnitude less than the value reported in nanoporous TiO_2.[73] The origin of a decrease of the resistivity was more complex for the following competing reasons: quite thin wall thickness, highly curved shape, extremely small contact area between the tubes and electrodes, and surface band bending by chemisorbed species on the surfaces of the tubes. The details will be published elsewhere.

Probing electrochemical properties of oxide nanotubes is also of importance for applications such as rechargeable lithium batteries and hydrogen-fuel generation. For vanadia nanotubes, their electrochemical properties have been well tested as cathode materials for lithium ion batteries by demonstrating the electrochemical charge/discharge cycling.[74] The typical capacity of the vanadia nanorolls ranged from 150 to 250 mAh g^{-1}. Recently, Sun et al. prepared the defect-rich nanorolls of vanadia under less reducing conditions and observed the increased capacity of 340 mAh g^{-1} and reproducible cyclic voltammograms, compared to crystalline V_2O_5.[75]

4.2. Optical Properties. Understanding the optical properties of oxide nanotubes could facilitates their sensory and display applications but is still in its infancy, demonstrating few studies in the literature. The observation of quantum confinements in oxide nanotubes has been a topic since the early synthesis of crystalline TiO_2 nanotubes.[8a,b] Sander et al. studied the optical properties of template-synthesized titania nanotubes and observed the blue shifts of the optical absorption edges with decreasing wall thickness.[28b] However, the spectral shifts could be attributed to the direct transition of electrons between interbands in this indirect band-gap semiconductor. Indeed, quantum size effects are expected in the size ranges of <1.5 nm for titania.[76]

Zhang et al. prepared a large number of silica nanotubes by the sol–gel template method and observed the strong photoluminescence from silica nanotubes in the visible region (Figure 6).[77] They have explained that the bright luminescence might be caused by the Si−OH complex on the silica nanotubes and the huge surface areas of both the inner and outer surfaces of the tubular structures. Liao et al. fabricated ZnO/ZnS nanotubes by sulfurating the surfaces of the template-directed ALD ZnO nanotubes in a solution of Na_2S.

They reported that the ZnO/ZnS core/sheath nanotubes having enhanced photoluminescent intensity of ultraviolet emission to deep-level emission is 9 times than that of the original ZnO nanotubes.[78]

4.3. Structural Properties. Unfortunately, as-prepared template-directed oxide nanotubes are mostly amorphous, except for a few examples such as vanadia nanotubes produced via rolling-up[55] and epitaxial[31c] growth. They can be transformed to polycrystalline phases by subsequent annealing at higher temperatures. Studies on the crystallization behavior of oxide nanotubes with a wall thickness of a few nanometers, which are lacking in the literature, are of importance scientifically as well as technologically. As for most applications, crystallized forms of nanotubes are required, for example, photovoltaic cells, catalysts, and sensors. On the other hand, the nanosized tubes' walls could show an intriguing size effect of the nucleation and grain growth during crystallization. Crystalline structures in nanowires where the grain boundaries are mostly oriented perpendicular or nearly perpendicular (called bamboo-like structures) show suppression of the grain growth because of their highly stable grain structure.[61] It could also be highly interesting to observe the grain growth in such oxide nanotubes.

5. Applications

5.1. Inorganic Drug-Delivery Agents. Colloidal particles with hollow cores in their interior have the ability of loading and releasing as well as transferring therapeutic agents and would enhance the therapeutic efficacy. Organic hollow particles such as colloidal-templated spheres, macroporous capsules, micelles, liposomes, and dendrimers have been the focus of this line of studies. Oxide nanotubes are another class of nanocontainers that would allow greater capability for this utility because of their biologically stable shell surfaces. Oxide surfaces exhibit stability superior to that of biological environments as a result of their slightly hydrophilic surface nature. That is, in the blood, plasma proteins called opsonins absorb onto the particles with hydrophobic surfaces, so that the particles covered by opsonins are cleared by the immune system; this is called the mononuclear phagocyte system or the reticuloendothelial system.[79] The other benefit of this oxide hollow system is that its hydroxyl surfaces are easy to tailor by a simple surface chemistry with a number of silane derivatives, indicating that specific biomolecules for the host–guest reactions as well as hydrophobic drugs for cancer therapy can be loaded into the interiors. In addition, multifunctional carriers should be realized by loading and/or coating the inside of oxide nanotubes with superparamagnetic nanoparticles (NPs) and/or fluorescent molecules.

Silica nanotubes are the most ideal candidate because they have the above advantages as well as a brittle shell, which may facilitate controlled release of the loaded species, for example, by the external stimulus such as ultrasound irradiation. The templated sol–gel silica nanotubes have been extensively studied by Martin and others. Mitchell et al. demonstrated that the inner and/or outer surfaces of silica nanotubes can be selectively functionalized to be hydrophobic and/or hydrophilic properties with dansylamide and octadecylsilanes.[80] Hillebrenner and co-workers showed that, by functionalization of the inside pores of silica nanotubes with aminosilane, aldehyde-functionalized polystyrene colloids can be selectively corked to the individual silica nanotubes by chemical self-assembly.[81]

Chen et al. showed that template-synthesized sol–gel silica nanotubes can deliver plasmid DNA into monkey kidney COS-7 cells.[82] They modified the inner surfaces of silica nanotubes with 3-(aminopropyl)trimethoxysilane in order to render positive charges and improve DNA loading. The DNA transfection to the COS-7 cells was monitored by the incorporation of CdSe/ZnS core/shell quantum dots into silica nanotubes. The transfection efficiency was reported to be 10–20%.

The toxicology of engineered nanomaterials for biomedical applications on the immune system is a recently emerging area and has been much less studied. A recent review paper deals with this topic, regarding the size, surface charge, and hydrophobicity of various kinds of nanomaterials.[83] For oxide systems, mesoporous silica spheres and crystalline TiO_2 have been tested for biomedical usage.[84] Although silica itself as a delivery agent has been proven in commerce, the shape effects of the nanotubes, e.g., high aspect ratio, on immunological impacts remain unknown.

5.2. Dye-Sensitized Solar Cells (DSSCs). Titania NPs have served as electron-harvesting and -transporting materials in conventional DSSCs, also known as the Grätzel cell.[85] TiO_2 NP films have large specific surface areas with a roughness factor of $\sim 10^3$. Grätzel and co-workers reported about 11% photoconversion efficiency of TiO_2 NP DSSCs. The factors that limit the DSSC performance is gained by theoretical cell efficiency. The photoconversion efficiency η of a solar cell is given by $\eta = (\mathrm{FF}|J_{SC}|V_{OC})/P_{in}$, where FF is the fill factor, $|J_{SC}|$ is the absolute value of the short-circuit current, V_{OC} is the open-circuit voltage, and P_{in} is the incident-light power density. The open-circuit voltage is determined by band gaps of the materials. The fill factor is determined by contact resistance. The short-circuit current is determined by the resistance of the materials and the amount of absorbed dye molecules. To increase the photoconversion efficiency of the DSSCs, the surface areas and conductivity of the materials should be enhanced. However, the randomly connected TiO_2 networks in NP DSSCs limit the efficient diffusion of the collected electrons to the outer electrodes.

Yang and co-workers made the ZnO nanowire DSSCs in which the traditional NP films were replaced by vertical arrays of crystalline ZnO nanowires.[86] The aspect ratio of the ZnO nanowires was ~120:1, and the longest nanowire arrays were 20−25 μm long. ZnO nanowire arrays were used as direct pathways for electrons and exhibited faster collection characteristics of charge carriers than NP networks through the device. However, the relatively low surface area associated with the roughness factor resulted in the small photoconversion efficiency of ~1.5% under Air Mass (AM) 1.5 Global solar conditions.

Oxide nanotube based DSSCs were recently proposed.[18] The dense arrays of nanotubes reach a roughness factor of $\sim 10^3$ or exceed the number in accordance with the length of the arrays. With TiO_2 nanotube DSSCs prepared using electrochemical anodization, a power conversion efficiency of about 3.2% was achieved by the Frank group.[18d] Very recently, Hupp and co-workers employed ZnO nanotubes as photoanodes in DSSCs. The ZnO nanotube arrays were fabricated on a 60-μm-thick membrane with 200 nm pores (Anodisc, Whatman) by the ALD technique. The power conversion efficiency was reported to be $\sim$1.6% under standard solar conditions.

Independently, we have recently prepared high-efficiency DSSCs based on the TiO_2 nanotube arrays. The TiO_2 nanotube arrays with crystalline anatase polymorphs were successfully formed by the template-directed ALD process. The physical dimensions of individual TiO_2 nanotubes were 2−20 nm wall thickness, 50−80 nm diameter, and 10−70 μm length. The density of the TiO_2 nanotube was $\sim 10^{10}$ #/cm^2, and the roughness factor was greater than 10^3. The enhanced power conversion efficiency could originate from the unique surface properties of our TiO_2 nanotubes, and the detailed scenario will be reported elsewhere.

5.3. Other Applications. The relatively large specific surface area, high aspect ratio structure, and transparent property of oxide nanotubes enable applications based on electrical and optical sensing. In addition to the above hydrogen sensor by the Grimes group, Chen et al. demonstrated that template-directed α-Fe_2O_3 nanotubes can be applied to gas sensors and lithium ion batteries.[87] Wang et al. prepared silica nanotubes by coaxial electrospinning and demonstrated that nanoscale channels ($\sim$20 nm) of silica nanotubes can serve as nanofluidic channels for single molecular detection.[88] Park et al. reported that anodized $TiO_{2-x}C_x$ nanotubes have shown more efficiency for photocatalytic water splitting than stoichiometric TiO_2 nanotubes and commercial TiO_2 NPs.[15] Kemell et al. studied the photocatalytic activity of TiO_2 nanotubes that have been fabricated by the template-directed ALD process and confirmed that the exposed surface area was essential to the photocatalytic performance.[49]

6. Concluding Remarks and Future Directions

In this review, we summarized the template-directed synthesis strategy for preparing oxide nanotubes, regarding template types. Positive and negative templating and quasi-templating processes provided unique structural characteristics of oxide nanotubes. Monodisperse samples of a wealth of oxide nanotubes possessing controllable wall thickness, diameter, and length could be obtained by combining porous membrane templates with ALD. Such a process might be expected as an ideal tool in the synthesis of oxide nanotubes, and its processing issues were discussed in terms of nanopore coating, selective etching, and dispersion. The fundamental chemical and physical properties of the template-synthesized oxide nanotubes were also summarized. We also discussed the potential for applications in drug-delivery systems, solar energy conversion devices, sensors, and photocatalysts.

As reviewed, there are relatively fewer publications on the studies of characterization and applications than those on the synthesis processes. Therefore, there would be many research opportunities that utilize those nanotubular structures of inorganic oxide. Characterization of the structural, electrical, and optical properties of individual and/or array oxide nanotubes has to be done for their unique applications. Wide ranges of potential applications need to be demonstrated from catalysts to electronic nanodevices because the template-directed methods can produce large quantities of oxide nanotubes. The ability to tailor the inner diameter of templated oxide nanotubes by controlling the wall thickness might also allow one to control the synthesis of a large number of nanowires with precisely tailored diameters in the sub-tens of nanometers length scale. For example, Bao et al. produced diameter-reduced Ni nanowires using a AAO membrane coated with sol–gel zirconia thin layers as the template and observed enhanced coercivity of this magnetic nanowire over that of the bulk Ni.[8g] Tan et al. recently achieved Au nanowires with controlled diameters in a certain range using the AAO template with ALD-coated silica films inside the pores.[50] In the near future, the template-directed technique will provide well-engineered oxide nanotubular-structured materials in large quantities as well as manufacturing tools for 1-D nanomaterials.

Acknowledgment. The authors thank Dr. Suh, Director of the Center for Nanostructured Materials Technology (CNMT), for his continuous encouragement and support. We acknowledge financial support by the CNMT under the 21 Century Frontier Research Programs of the Korea government (MOST; Grant M105KO010026-07K1501-02610), the National Research Lab Programs of the Korea Science and Engineering Foundation (KOSEF) and MOST (Grant R0A-2007-000-20105-0), and the Engineering Research Center Programs of MOST/KOSEF (Center for Materials and Processes of Self-Assembly; Grant R11-2005-048-00000-0). C.B. is a National Science Scholar of KOSEF (2007−2008; S2-2007-000-00061-1) and a Seoul Science Fellow of Seoul City, Korea (2006−2007).

References

(1) Reviews: (a) Martin, C. R. *Science* **1994**, *266*, 1961. (b) Martin, C. R. *Acc. Chem. Res.* **1995**, *28*, 61. (c) Martin, C. R. *Chem. Mater.* **1996**, *8*, 1739.
(2) Iijima, S. *Nature* **1991**, *354*, 56.
(3) Reviews: (a) Ajayan, P. M. *Chem. Rev.* **1999**, *99*, 1787. (b) Baughman, R. H.; Zakhidov, A. A.; de Heer, W. A. *Science* **2002**, *297*, 787.
(4) Special issues: (a) *Acc. Chem. Res.* **2002**, *35*, 997. (b) *Chem. Vap. Deposition* **2006**, *12*, 307.
(5) For example, (a) Parthasarathy, R. V.; Martin, C. R. *Chem. Mater.* **1994**, *6*, 1627. (b) Steinhart, M.; Wendorff, J. H.; Greiner, A.; Wehrspohn, R. B.; Nielsch, K.; Schilling, J.; Choi, J.; Gösele, U. *Science* **2002**, *297*, 1997. (c) Steinhart, M.; Wehrspohn, R. B.; Gosele, U.; Wendorff, J. H. *Angew. Chem., Int. Ed.* **2004**, *43*, 1334. (d) Aleshin, A. N. *Adv. Mater.* **2006**, *18*, 17. (e) De Vito, S.; Martin, C. R. *Chem. Mater.* **1998**, *10*, 1738. (f) Cepak, V. M.; Martin, C. R. *Chem. Mater.* **1999**, *11*, 1363.
(6) For example, (a) Nishizawa, M.; Menon, V. P.; Martin, C. R. *Science* **1995**, *268*, 700. (b) Jirage, K. B.; Hulteen, J. C.; Martin, C. R. *Science* **1997**, *278*, 655. (c) Sun, Y.; Mayers, B. T.; Xia, Y. *Nano Lett.* **2002**, *2*, 481. (d) Sun, Y.; Mayers, B. T.; Xia, Y. *Adv. Mater.* **2003**, *15*, 641. (e) Wirtz, M.; Martin, C. R. *Adv. Mater.* **2003**, *15*, 455. (f) Mu, C.; Yu, Y.-X.; Wang, R. M.; Wu, K.; Xu, D. S.; Guo, G.-L. *Adv. Mater.* **2004**, *16*, 1550. (g) Qu, L.; Shi, G.; Wu, X.; Fan, B. *Adv. Mater.* **2004**, *16*, 1200. (h) Sanchez-Castillo, M. A.; Couto, C.; Kim, W. B.; Dumesic, J. A. *Angew. Chem., Int. Ed.* **2004**, *43*, 1140. (i) Kijima, T.; Yoshimura, T.; Uota, M.; Ikeda, T.; Fujikawa, D.; Mouri, S.; Uoyama, S. *Angew. Chem., Int. Ed.* **2004**, *43*, 228. (j) Lee, W.; Scholz, R.; Nielsch, K.; Gosele, U. *Angew. Chem., Int. Ed.* **2004**, *44*, 6050. (k) Lahav, M.; Weiss, E. A.; Xu, Q.; Whitesides, G. M. *Nano Lett.* **2006**, *6*, 2166.

(7) (a) Hoyer, P. *Langmuir* **1996**, *12*, 1411. (b) Hoyer, P. *Adv. Mater.* **1996**, *8*, 857.

(8) (a) Lakshmi, B. B.; Patrissi, C. J.; Martin, C. R. *Chem. Mater.* **1997**, *9*, 2544. (b) Lakshmi, B. B.; Dorhout, P. K.; Martin, C. R. *Chem. Mater.* **1997**, *9*, 857. (c) Imai, H.; Takei, Y.; Shimizu, K.; Matsuda, M.; Hirashima, H. *J. Mater. Chem.* **1999**, *9*, 2971. (d) Kobayashi, S.; Hanabusa, K.; Hamasaki, N.; Kimura, M.; Shirai, H.; Shinkai, S.; Shinkai, S. *Chem. Mater.* **2000**, *12*, 1523. (e) Imai, H.; Matsuta, M.; Shimizu, K.; Hirashima, H.; Negishi, N. *J. Mater. Chem.* **2000**, *10*, 2005. (f) Caruso, R. A.; Schattka, J. H.; Greiner, A. *Adv. Mater.* **2001**, *13*, 1577. (g) Bao, J.; Xu, D.; Zhou, Q.; Xu, Z.; Feng, Y.; Zhou, Y. *Chem. Mater.* **2002**, *14*, 4709. (h) Chu, S. Z.; Wada, K.; Inoue, S. *Adv. Mater.* **2002**, *14*, 1752. (i) Michailowski, A.; AlMawlawi, D.; Cheng, G.; Moskovits, M. *Chem. Phys. Lett.* **2001**, *349*, 1. (j) Cheng, B.; Samulski, E. T. *J. Mater. Chem.* **2001**, *11*, 2901. (k) Hernandez, B. A.; Chang, K.-S.; Fisher, E. R.; Dorhout, P. K. *Chem. Mater.* **2002**, *14*, 480. (l) Gasparac, R.; Kohli, P.; Mota, M. O.; Trofin, L.; Martin, C. R. *Nano Lett.* **2004**, *4*, 513.

(9) (a) Kasuga, T.; Hiramatsu, M.; Hoson, A.; Sekino, T.; Niihara, K. *Langmuir* **1998**, *14*, 3160. (b) Kasuga, T.; Hiramatsu, M.; Hoson, A.; Sekino, T.; Niihara, K. *Adv. Mater.* **1999**, *11*, 1307. (c) Du, G. H.; Chen, Q.; Che, R. C.; Yuan, Z. Y.; Peng, L.-M. *Appl. Phys. Lett.* **2001**, *79*, 3702. (d) Chen, Q.; Zhou, W.; Du, G. H.; Peng, L.-M. *Adv. Mater.* **2002**, *14*, 1208. (e) Yao, B. D.; Chan, Y. F.; Zhang, X. Y.; Zhang, W. F.; Yang, Z. Y.; Wang, N. *Appl. Phys. Lett.* **2003**, *82*, 281. (f) Tian, Z. R.; Voigt, J. A.; Liu, J.; Mckenzie, B.; Xu, H. *J. Am. Chem. Soc.* **2003**, *125*, 12384. (h) Poudel, B.; Wang, W. Z.; Dames, C.; Huang, J. Y.; Kunwar, S.; Wang, D. Z.; Banerjee, D.; Chen, G.; Ren, Z. F. *Nanotechnol.* **2005**, *16*, 1935. (i) Bavykin, D. V.; Friedrich, J. M.; Walsh, F. C. *Adv. Mater.* **2006**, *18*, 2807.

(10) (a) Zwilling, V.; Aucouturier, M.; Darque-Ceretii, E. *Electrochim. Acta* **1999**, *45*, 921. (b) Gong, D.; Grimes, C. A.; Varghese, O. K.; Hu, W.; Singh, R. S.; Chen, Z.; Dickey, E. C. *J. Mater. Res.* **2001**, *16*, 3331. (c) Pu, L.; Bao, X.; Zou, J.; Feng, D. *Angew. Chem., Int. Ed.* **2001**, *40*, 1490. (d) Beranek, R.; Hildebrand, H.; Schmuki, P. *Electrochem. Solid-State Lett.* **2003**, *6*, B12. (e) Macak, J. M.; Tsuchiya, H.; Schmuki, P. *Angew. Chem., Int. Ed.* **2005**, *44*, 2100. (f) Macak, J. M.; Tsuchiya, H.; Taveira, L.; Aldabergerova, S.; Schmuki, P. *Angew. Chem., Int. Ed.* **2005**, *44*, 7463. (g) Richter, C.; Wu, Z.; Panaitescu, E.; Willey, R. J.; Menon, L. *Adv. Mater.* **2007**, *19*, 946. (h) Albu, S. P.; Ghicov, A.; Macak, J. M.; Schmuki, P. *Phys. Status Solidi* **2007**, *1*, R65. (i) Ruan, C.; Paulose, M.; Varghese, O. K.; Mor, G. K.; Grimes, C. A. *J. Phys. Chem., B* **2005**, *109*, 15754. (j) Paulose, M.; Shankar, K.; Yoriya, S.; Prakasam, H. E.; Varghese, O. K.; Mor, G. K.; Latempa, T. A.; Fitzgerald, A.; Grimes, C. A. *J. Phys. Chem., B* **2005**, *110*, 16179. (k) Shankar, K.; Mor, G. K.; Fitzgerald, A.; Grimes, C. A. *J. Phys. Chem., C* **2007**, *111*, 21. (l) Shankar, K.; Mor, G. K.; Prakasam, H. E.; Yoriya, S.; Paulose, M.; Varghese, O. K.; Grimes, C. A. *Nanotechnol.* **2007**, *18*, 65707.

(11) Martin, C. R.; Kohli, P. *Nat. Rev. Drug Discovery* **2003**, *2*, 29.

(12) Lee, S. B.; Mitchell, D. T.; Trofin, L.; Nevanen, T. K.; Söderlund, H.; Martin, C. R. *Science* **2002**, *296*, 2198.

(13) Fan, R.; Karnik, R.; Yue, M.; Li, D.; Majumdar, A.; Yang, P. *Nano Lett.* **2005**, *5*, 1633.

(14) Quan, X.; Yang, S.; Ruan, X.; Zhao, H. *Environ. Sci. Technol.* **2005**, *39*, 3770.

(15) Park, J.; Kim, H. S.; Bard, A. J. *Nano Lett.* **2006**, *6*, 24.

(16) (a) Varghese, O. K.; Gong, D.; Paulose, M.; Ong, K. G.; Grimes, C. A. *Sens. Actuators, B* **2003**, *93*, 338. (b) Varghese, O. K.; Gong, D.; Paulose, M.; Ong, K. G.; Dickey, E. C.; Grimes, C. A. *Adv. Mater.* **2003**, *15*, 624.

(17) (a) Uchida, S.; Chiba, R.; Tomiha, M.; Masaki, N.; Shirai, M. *Electrochem.* **2002**, *70*, 418. (b) Ohsaki, Y.; Masaki, N.; Kitamura, T.; Wada, Y.; Okamoto, T.; Sekino, T.; Niihara, K.; Yanagida, S. *Phys. Chem. Chem. Phys.* **2005**, *7*, 4157.

(18) (a) Macak, J. M.; Tsuchiya, H.; Ghicov, A.; Schmuki, P. *Electrochem. Commun.* **2005**, *7*, 1133. (b) Paulose, M.; Shankar, K.; Varghese, O. K.; Mor, G. K.; Hardin, B.; Grimes, C. A. *Nanotechnol.* **2006**, *17*, 1446. (c) Mor, G. K.; Shankar, K.; Paulose, M.; Varghese, O. K.; Grimes, C. A. *Nano Lett.* **2006**, *6*, 215. (d) Zhu, K.; Neale, N. R.; Miedaner, A.; Frank, A. J. *Nano Lett.* **2007**, *7*, 69. (e) Martinson, A. B. F.; Elam, J. W.; Hupp, J. T.; Pellin, M. J. *Nano Lett.* **2007**, *7*, 2183.

(19) (a) Adachi, M.; Murata, Y.; Harada, M.; Yoshikawa, S. *Chem. Lett.* **2000**, *29*, 942. (b) Adachi, M.; Okada, I.; Ngamsinlapasathian, S.; Murata, Y.; Yoshikawa, S. *Electrochemistry* **2002**, *70*, 449. (c) Adachi, M.; Murata, Y.; Okada, I.; Yoshikawa, S. *J. Electrochem. Soc.* **2003**, *150*, G488. (d) Ngamsinlapasathian, S.; Sakulkhaemaruethai, S.; Pavasupree, S.; Kitiyanan, A.; Sreethawong, T.; Suzuki, Y.; Yoshikawa, S. *J. Photochem. Photobiol., A* **2004**, *164*, 145.

(20) (a) Nemetschek, Th.; Hofmann, U. *Z. Naturforsch.* **1953**, *8b*, 410. (b) Nemetschek, Th.; Hofmann, U. *Z. Naturforsch.* **1954**, *9b*, 166.

(21) (a) Saupe, G. B.; Waraksa, C. C.; Kim, H.-N.; Han, Y. J.; Kaschak, D. M.; Skinner, D. M.; Mallouk, T. E. *Chem. Mater.* **2000**, *12*, 1556. (b) Wang, Z. L.; Gao, R. P.; Gole, J. L.; Stout, J. D. *Adv. Mater.* **2000**, *12*, 1938. (c) Kobayashi, Y.; Hata, H.; Salama, M.; Mallouk, T. E. *Nano Lett.* **2007**, *7*, 2142. (d) Hu, J.-Q.; Meng, X.-M.; Jiang, Y.; Lee, C.-S.; Lee, S.-T. *Adv. Mater.* **2003**, *15*, 70. (e) Li, Y.; Bando, Y.; Golberg, D. *Adv. Mater.* **2003**, *15*, 581. (f) Li, Y.; Bando, Y.; Golberg, D. *Adv. Mater.* **2003**, *16*, 37. (g) Hu, J.; Bando, Y.; Golberg, D.; Liu, Q. *Angew. Chem., Int. Ed.* **2003**, *42*, 3493. (h) Liu, Y.; Dong, J.; Liu, M. *Adv. Mater.* **2004**, *16*, 353. (i) Liu, Y.; Liu, M. *Adv. Funct. Mater.* **2005**, *15*, 57.

(22) (a) Reviews: Li, D.; Xia, Y. *Adv. Mater.* **2004**, *16*, 1151. (b) Li, D.; McCann, J. T.; Marquez, M.; Xia, Y. *J. Am. Ceram. Soc.* **2006**, *89*, 1861.

(23) (a) Obare, S. O.; Jana, N. R.; Murphy, C. J. *Nano Lett.* **2001**, *1*, 601. (b) Mayya, K. S.; Gittins, D. I.; Dibaj, A. M.; Caruso, F. *Nano Lett.* **2001**, *1*, 727. (c) Zygmunt, J.; Krumeich, F.; Nesper, R. *Adv. Mater.* **2003**, *15*, 1538. (d) Lee, J.-H.; Leu, I.-C.; Hsu, M.-C.; Chung, Y.-W.; Hon, M.-H. *J. Phys. Chem., B* **2005**, *109*, 13056.

(24) Fan, R.; Wu, Y.; Li, D.; Yue, M.; Majumdar, A.; Yang, P. *J. Am. Chem. Soc.* **2003**, *125*, 5254.

(25) Li, L.; Yang, Y.-W.; Li, G.-H.; Zhang, L.-D. *Small* **2006**, *2*, 548.

(26) Gao, P. X.; Lao, C. S.; Ding, Y.; Wang, Z. L. *Adv. Funct. Mater.* **2006**, *16*, 53.

(27) (a) Baral, S.; Schoen, P. *Chem. Mater.* **1993**, *5*, 145. (b) Adachi, M.; Harada, T.; Harada, M. *Langmuir* **1999**, *15*, 7097. (c) Harada, M.; Adachi, M. *Adv. Mater.* **2000**, *12*, 839. (d) Ono, Y.; Kanekiyo, Y.; Inoue, K.; Hojo, J.; Nango, M.; Shinkai, S. *Chem. Lett.* **1999**, *6*, 475. (e) Ono, Y.; Nakashima, K.; Sano, M.; Hojo, J.; Shinkai, S. *Chem. Lett.* **1999**, *10*, 1119. (f) Ji, Q.; Iwaura, R.; Shimizu, T. *Chem. Lett.* **2004**, *33*, 504. (g) Ji, Q.; Iwaura, R.; Kogiso, M.; Jung, J. H.; Yoshida, K.; Shimizu, T. *Chem. Mater.* **2004**, *16*, 250. (h) Meegan, J. E.; Aggeli, A.; Boden, N.; Brydson, R.; Brown, A. P.; Carrick, L.; Brough, A. R.; Hussain, A.; Ansell, R. J. *Adv. Funct. Mater.* **2004**, *14*, 31. (i) Yuwono, V. M.; Hartgerink, J. D. *Langmuir* **2007**, *23*, 5033. (j) Zhang, Z.; Buitenhuis, J. *Small* **2007**, *3*, 424.

(28) (a) Shin, H.; Jeong, D.-K.; Lee, J.; Sung, M. M.; Kim, J. *Adv. Mater.* **2004**, *16*, 1197. (b) Sander, M. S.; Côté, M. J.; Gu, W.; Kile, B. M.; Tripp, C. P. *Adv. Mater.* **2004**, *16*, 2052.

(29) (a) Hwang, J.; Min, B.; Lee, J. S.; Keem, K.; Cho, K.; Sung, M.-Y.; Lee, M.-S.; Kim, S. *Adv. Mater.* **2004**, *16*, 422. (b) Peng, Q.; Sun, X.-Y.; Spagnola, J. C.; Hyde, G. K.; Spontak, R. J.; Parsons, G. N. *Nano Lett.* **2007**, *7*, 719. (c) Wang, C.-C.; Kei, C.-C.; Yu, Y.-W.; Perng, T.-P. *Nano Lett.* **2007**, *7*, 1566. (d) Ras, R. H. A.; Kemell, M.; de Wit, J.; Ritala, M.; ten Brinke, G.; Leskela, M.; Ikkala, O. *Adv. Mater.* **2007**, *19*, 102.

(30) (a) Daub, M.; Knez, M.; Gosele, U.; Nielsch, K. *J. Appl. Phys.* **2007**, *101*, 09J111. (b) Kemell, M.; Pore, V.; Tupala, J.; Ritala, M.; Leskela, M. *Chem. Mater.* **2007**, *19*, 1816.

(31) (a) Nakamura, H.; Matsui, Y. *J. Am. Chem. Soc.* **1995**, *117*, 2651. (b) Nakamura, H.; Matsui, Y. *Adv. Mater.* **1995**, *7*, 871. (c) Ajayan, P. M.; Stephan, O.; Redlich, P. H.; Colliex, C. *Nature* **1995**, *375*, 564.

(32) Rao, C. N. R.; Satishkumar, B. C.; Govindaraj, A. *Chem. Commun.* **1997**, 1581.

(33) Melechko, V.; McKnight, T. E.; Guillorn, M. A.; Austin, D. W.; Ilic, B.; Merkulov, V. I.; Doktycz, M. J.; Lowndes, D. H.; Simpson, M. L. *J. Vac. Sci. Technol., B* **2002**, *20*, 2730.

(34) (a) Lee, J. S.; Min, B.; Cho, K.; Kim, S.; Park, J.; Lee, Y. T.; Kim, N. S.; Lee, M. S.; Park, S. O.; Moon, J. T. *J. Cryst. Growth* **2003**, *254*, 443. (b) Herrmann, C. F.; Fabreguette, F. H.; Finch, D. S.; Geiss, R.; George, S. M. *Appl. Phys. Lett.* **2005**, *87*, 123110. (c) Farmer, D.; Gordon, R. G. *Electrochem. Solid-State Lett.* **2005**, *8*, G89. (d) Farmer, D. B.; Gordon, R. G. *Nano Lett.* **2006**, *6*, 699. (e) Lu, Y.; Bangsaruntip, S.; Wang, X.; Zhang, L.; Nishi, Y.; Dai, H. *J. Am. Chem. Soc.* **2006**, *128*, 3518.

(35) Fan, H. J.; Knez, M.; Scholz, R.; Nielsch, K.; Pippel, E.; Hesse, D.; Zacharias, M.; Gosele, U. *Nat. Mater.* **2006**, *5*, 627.

(36) Alexe, M.; Hesse, D.; Schmidt, V.; Senz, S.; Fan, H. J.; Zacharias, M.; Gosele, U. *Appl. Phys. Lett.* **2006**, *89*, 172907.

(37) Caruso, R. A.; Schattka, J. H.; Greiner, A. *Adv. Mater.* **2001**, *13*, 1577.

(38) Lowenstam, H. A.; Weiner, S. *On Biomineralization*; Oxford University Press: London, 1989.

(39) Kobayashi, S.; Hamasaki, N.; Suzuki, M.; Kimura, M.; Shirai, H.; Hanabusa, K. *J. Am. Chem. Soc.* **2002**, *124*, 6550.

(40) Ji, Q.; Iwaura, R.; Shimizu, T. *Chem. Mater.* **2007**, *19*, 1329.

(41) Jung, J. H.; Kobayashi, H.; van Bommel, K. J. C.; Shinkai, S.; Shimizu, T. *Chem. Mater.* **2002**, *14*, 1445.

(42) Yada, M.; Mihara, M.; Mouri, S.; Kuroki, M.; Kijima, T. *Adv. Mater.* **2002**, *14*, 309.

(43) (a) Kovtyukhova, N. I.; Mallouk, T. E.; Mayer, T. S. *Adv. Mater.* **2003**, *15*, 780. (b) Hou, S.; Harrell, C. C.; Trofin, L.; Kohli, P.; Martin, C. R. *J. Am. Chem. Soc.* **2004**, *126*, 5674. (c) Kohli, P.; Martin, C. R. *Curr. Pharm. Biotechnol.* **2005**, *6*, 35.

(44) Sander, M. S.; Cote, M. J.; Gu, W.; Kile, B. M.; Tripp, C. P. *Adv. Mater.* **2004**, *16*, 2052.

(45) Scholes, G. D.; Rumbles, G. *Nat. Mater.* **2006**, *5*, 683.

(46) Kim, C.; Lee, B.; Yang, H. J.; Lee, H. M.; Lee, J. G.; Shin, H. *J. Kor. Phys. Soc.* **2005**, *47*, S417.

(47) (a) Shen, X.-P.; Liu, H.-J.; Pan, L.; Chen, K.-M.; Hong, J.-M.; Xu, Z. *Chem. Lett.* **2004**, *33*, 1128. (b) Malandrino, G.; Finocchiaro, S. T.; Lo Nigro, R.; Bongiorno, C.; Spinella, C.; Fragala, I. L. *Chem. Mater.* **2004**, *16*, 5559. (c) Shen, X.-P.; Liu, H.-J.; Fan, X.; Hong, J.-M. *J. Cryst. Growth* **2005**, *276*, 471. (d) Malandrino, G.; Perdicaro, L. M. S.; Fragala, I. L.; Lo Nigro, R.; Losurdo, M.; Bruno, G. J. *Phys. Chem. C* **2007**, *111*, 3211.

(48) Daub, M.; Knez, M.; Göesele, U.; Nielsch, K. *J. Appl. Phys.* **2007**, *101*, 9J111.

(49) Kemell, M.; Pore, V.; Tupala, J.; Ritala, M.; Leskela, M. *Chem. Mater.* **2007**, *19*, 1816.

(50) Tan, L. K.; Chong, A. S. M.; Tang, X. S. E.; Gao, H. *J. Phys. Chem., C* **2007**, *111*, 4964.

(51) A review: Xia, Y.; Whitesides, G. M. *Angew. Chem., Int. Ed.* **1998**, *37*, 550.

(52) (a) Tsuchiya, H.; Macak, J. M.; Sieber, I.; Schmuki, P. *Small* **2005**, *1*, 722. (b) Ghicov, A.; Aldabergerova, S.; Tsuchiya, H.; Schmuki, P. *Angew. Chem., Int. Ed.* **2006**, *45*, 6993. (c) Yasuda, K.; Schmuki, P. *Adv. Mater.* **2007**, *19*, 1757.

(53) Pu, L.; Bao, X.; Zou, J.; Feng, D. *Angew. Chem., Int. Ed.* **2001**, *40*, 1490.
(54) Loscertales, I. G.; Barrero, A.; Márquez, M.; Spretz, R.; Velarde-Ortiz, R.; Larsen, G. *J. Am. Chem. Soc.* **2004**, *126*, 5376.
(55) (a) Spahr, M. E.; Bitterli, P.; Nesper, R.; Müller, M.; Krumeich, F. H.; Nissen, U. *Angew. Chem., Int. Ed.* **1998**, *37*, 1263. (b) Krumeich, F.; Muhr, H.-J.; Niederberger, M.; Bieri, F.; Schnyder, B.; Nesper, R. *J. Am. Chem. Soc.* **1999**, *121*, 8324. (c) Muhr, H.-J.; Krumeich, F.; Schönholzer, U. P.; Bieri, F.; Niederberger, M.; Gauckler, L. J.; Nesper, R. *Adv. Mater.* **2000**, *12*, 231. (d) Tang, C. C.; Bando, Y.; Liu, B. D.; Golberg, D. *Adv. Mater.* **2005**, *17*, 3005. (e) Jia, C.-J.; Sun, L.-D.; Yan, Z.-G.; You, L.-P.; Luo, F.; Han, X.-D.; Pang, Y.-C.; Zhang, Z.; Yan, C.-H. *Angew. Chem., Int. Ed.* **2005**, *44*, 4328. (f) Nordlinder, S.; Nyholm, L.; Gustafsson, T.; Edstrom, K. *Chem. Mater.* **2006**, *18*, 495. (g) Patzke, G. R.; Krumeich, F.; Nesper, R. *Angew. Chem., Int. Ed.* **2002**, *41*, 2446.
(56) Pouget, E.; Dujardin, E.; Cavalier, A.; Moreac, A.; Valery, C.; Marchi-Artzner, V.; Weiss, T.; Renault, A.; Paternostre, M.; Artzner, F. *Nat. Mater.* **2007**, *6*, 434.
(57) Ugarte, D.; Châtelain, A.; de Heer, W. A. *Science* **1996**, *274*, 1879.
(58) Okamoto, K.; Shook, C. J.; Bivona, L.; Lee, S. B.; English, D. S. *Nano Lett.* **2004**, *4*, 233.
(59) Elam, J. W.; Routkevitch, D.; Mardilovich, P. P.; George, S. M. *Chem. Mater.* **2003**, *15*, 3507.
(60) From the ideal gas law, we can estimate the mean free path of the precursor molecules in our system λ as $RTl(2^{1/2}\pi d^2 N_A P)$ where R is the gas constant, T is the temperature, d is the molecular diameter, N_A is Avogadro's number, and P is the pressure.
(61) Sander, M. S.; Gronsky, R.; Sands, T.; Stacy, A. M. *Chem. Mater.* **2003**, *15*, 335.
(62) Groner, M. D.; Fabreguette, F. H.; Elam, J. W.; George, S. M. *Chem. Mater.* **2004**, *16*, 639.
(63) Jones, D. A. *Principles and prevention of corrosion*, 2nd ed.; Prentice Hall: Upper Saddle River, NJ, 1996; p 61.
(64) Xiong, G.; Elam, J. W.; Feng, H.; Han, C. Y.; Wang, H.-H.; Iton, L. E.; Curtiss, L. A.; Pellin, M. J.; Kung, M.; Kung, H.; Stair, P. C. *J. Phys. Chem., B* **2005**, *109*, 14059.
(65) Dushkin, C. D.; Kralchevsky, P. A.; Yoshimura, H.; Nagayama, K. *Phys. Rev. Lett.* **1995**, *75*, 3454.
(66) Breen, T. L.; Tien, J.; Oliver, S. R.; Hadzic, T.; Whitesides, G. M. *Science* **1999**, *284*, 948.
(67) Park, S.; Lim, J.-H.; Chung, S.-W.; Mirkin, C. A. *Science* **2004**, *303*, 348.
(68) (a) Chiang, Y. M.; Lavik, E. B.; Kosacki, I.; Tuller, H. L.; Ying, J. Y. *Appl. Phys. Lett.* **1996**, *69*, 185. (b) Kosacki, I.; Suzuki, T.; Petrovsky, V.; Anderson, H. U. *Solid State Ionics* **2000**, *136*, 1225. (c) Knauth, P.; Tuller, H. L. *J. Appl. Phys.* **1999**, *85*, 897.
(69) Cha, D. K.; Lee, B.; Huang, J.; Kim, J.; Wallace, R. M.; Gnade, B. E.; Kim, M. J. *Microsc. Microanal.* **2006**, *12*, 1272.
(70) Diebold, U. *Surf. Sci. Rep.* **2003**, *48*, 53.
(71) (a) Tang, H.; Lévy, F.; Berger, H.; Schmid, P. E. *Phys. Rev. B* **1995**, *52*, 7771. (b) Könenkamp, R. *Phys. Rev. B* **2000**, *61*, 11057.
(72) Papadopoulos, C.; Rakitin, A.; Li, J.; Vedeneev, A. S.; Xu, J. M. *Phys. Rev. Lett.* **2000**, *851*, 3476.
(73) Dittrich, T.; Weidmann, J.; Koch, F.; Uhlendorf, I.; Lauermann, I. *Appl. Phys. Lett.* **1999**, *75*, 3980.
(74) (a) Dobley, A.; Ngala, K.; Yang, S.; Zavalij, P. Y.; Whittingham, M. S. *Chem. Mater.* **2001**, *13*, 4382. (b) Nordlinder, S.; Edstrom, K.; Gustafsson, T. *Electrochem. Solid-State Lett.* **2001**, *4*, A129. (c) Spahr, M. E.; Stoschitzki-Bitterli, P.; Nesper, R.; Haas, O.; Novak, P. *J. Electrochem. Soc.* **1999**, *146*, 2780.
(75) Sun, D.; Kwon, C. W.; Baure, G.; Richman, E.; MacLean, J.; Dunn, B.; Tolbert, S. H. *Adv. Funct. Mater.* **2004**, *14*, 1197.
(76) Monticone, S.; Tufeu, R.; Kanaev, A. V.; Scolan, E.; Sanchez, C. *Appl. Surf. Sci.* **2000**, *162–163*, 565.
(77) Zhang, M.; Ciocan, E.; Bando, Y.; Wada, K.; Cheng, L. L.; Pirouz, P. *App. Phys. Lett.* **2002**, *80*, 491.
(78) Liao, H.-C.; Kuo, P.-C.; Lin, C.-C.; Chen, S.-Y. *J. Vac. Sci. Technol., B* **2006**, *24*, 2198.
(79) Guo, X. In *Design of Controlled Release Drug Delivery Systems*; LiX. Jasti, B. R., Eds.; McGraw-Hill: New York, 2006; Chapter11, pp 339–374.
(80) Mitchell, D. T.; Lee, S. B.; Trofin, L.; Li, N.; Nevanen, T. K.; Soderlund, H.; Martin, C. R. *J. Am. Chem. Soc.* **2002**, *124*, 11864.
(81) Hillebrenner, H.; Buyukserin, F.; Kang, M.; Mota, M. O.; Stewart, J. D.; Martin, C. R. J. *Am. Chem. Soc.* **2006**, *128*, 4236.
(82) Chen, C.-C.; Liu, Y.-C.; Wu, C.-H.; Yeh, C.-C.; Su, M.-T.; Wu, Y.-C. *Adv. Mater.* **2005**, *17*, 404.
(83) Dobrovolskaia, M. A.; McNeil, S. E. *Nat. Nanotechnol.* **2007**, *2*, 269.
(84) (a) Radu, D. R.; Lai, C.-Y.; Jeftinija, K.; Rowe, E. W.; Jeftinija, S.; Lin, V. S.-Y. *J. Am. Chem. Soc.* **2004**, *126*, 13216. (b) Vallhov, H.; Gabrielsson, S.; Stromme, M.; Scheynius, A.; Garcia-Bennett, A. E. *Nano Lett.* DOI: 10.1021/nl0714785. (c) Sayes, C. M.; Wahi, R.; Kurian, P. A.; Liu, Y. P.; West, J. L.; Ausman, K. D.; Warheit, D. B.; Colvin, V. L. *Toxicol. Sci.* **2006**, *92*, 174.
(85) O'Regan, B.; Grätzel, M. *Nature.* **1991**, *353*, 737.
(86) Law, M.; Greene, L. E.; Johnson, J. C.; Saykally, R.; Yang, P. *Nat. Mater.* **2005**, *4*, 455.
(87) Chen, J.; Xu, L.; Li, W.; Gou, X. *Adv. Mater.* **2005**, *17*, 582.
(88) Wang, M.; Jing, N.; Su, C. B.; Kameoka, J.; Chou, C.-K.; Hung, M.-C.; Chang, K.-A. *Appl. Phys. Lett.* **2006**, *88*, 33106.
(89) Bae, C.; Shin, H. 2008 in preparation.

CM702138C